

Fabrication and Experimental Testing of Variable-View Factor Two-Phase Radiators

Jeff Diebold¹, Calin Tarau², Andrew Lutz³ and Srujan Rokkam⁴
Advanced Cooling Technologies, Inc., Lancaster, PA, 17601

Michael Eff⁵ and Lindsey Lindamood⁶
Edison Welding Institute, Columbus, OH, 43221

In order to address the need for light-weight, deployable and efficient radiators capable of passive thermal control and a significant heat rejection turndown ratio, Advanced Cooling Technologies, Inc. (ACT) has developed a novel vapor-pressure-driven variable-view-factor and deployable radiator that passively operates with variable geometry (i.e., view factor). The device utilizes two-phase heat transfer and novel geometric features that passively (and reversibly) adjust the view factor in response to the internal vapor pressure in the radiator. This paper presents the results of the successful collaboration between ACT and the Edison Welding Institute (EWI) to fabricate the variable view factor two phase radiator (VVFTPR) from aluminum 7075 via ultrasonic welding. The various steps of the manufacturing process are described, followed by experimental testing of the prototypes. Operation of an ultrasonically welded VVFTPR in response to changes in the vapor pressure of a two-phase working fluid was successfully demonstrated.

I. Introduction

All manned spacecraft, satellites, and unmanned spacecraft need to reject waste heat by radiating heat through a radiator, while maintaining the battery and electronics temperatures within specified limits. The amount of waste heat, and the heat sink conditions can vary widely, e.g., when a satellite moves behind the earth. Typically, radiators are sized for the highest power at the hottest sink conditions, so they are oversized for most scenarios. Hence, there is a need to develop light-weight and efficient radiators for future spacecraft and satellites which offers the capability of significant turndown.^{1,2}

Under a Small Business Innovation Research (SBIR) project funded by NASA Marshall Space Flight Center, Advanced Cooling Technologies, Inc. (ACT) developed a novel *vapor-pressure-driven variable-view-factor and deployable radiator* that passively operates with variable geometry (i.e., view factor) and offers high heat rejection turndown ratio. The advantages of the variable-view-factor two-phase radiator (VVFTPR) over a conventional flat panel radiator include:

- *Passive temperature control*: Variable thermal resistance minimizes temperature swings despite changes in operating or environmental conditions. This feature will maintain the electronics above the minimum operating temperature even during times of low heat loads and low heat sink temperatures.
- *Survival*: In the fully closed position, heat rejection from the radiator is minimized resulting in a reduction in the required survival heater power.
- *Deployable*: During launch the radiator is in a compact configuration allowing for simplified storage.

The VVFTPR concept has been developed through a Phase I and II SBIR program and progress has been documented in several publications. Lutz et al.³ presented the concept of the VVFTPR and developed a successful

¹ R&D Engineer II, R&D, 1046 New Holland Ave.

² Principal Engineer, R&D, 1046 New Holland Ave.

³ R&D Engineer III, R&D, 1046 New Holland Ave.

⁴ Lead Engineer, R&D, 1046 New Holland Ave.

⁵ Senior Engineer, 1250 Arthur E. Adams Dr.

⁶ Applications Engineer, 1250 Arthur E. Adams Dr.

prototype. Diebold et al.⁴ presented 3D structural simulations used for trade studies to investigate the effects of internal pressure and VVFTPR geometry on radiator view factor. The results of the structural simulations were used to develop a thermal model demonstrating the thermal control capability of the VVFTPR. In a subsequent publication, Diebold et al.⁵ discussed manufacturing challenges and preliminary work to fabricate VVFTPR panels from aluminum 7075 using ultrasonic welding. ACT began collaborating with Edison Welding Institute (EWI), a company that specializes in advanced manufacturing techniques, to develop an ultrasonic welding process applicable to the VVFTPR. This paper will discuss progress on manufacturing and experimental testing of ultrasonically welded VVFTPR prototypes.

II. Variable View Factor Concept

The basic concept of the VVFTPR is illustrated in Figure 1a. The flexible actuator section of the VVFTPR consists of a hollow curved panel that is filled with a two-phase working fluid and sealed. An increase in fluid temperature results in a higher vapor pressure within the hollow curved panel causing the radiator to open. This opening increases the effective view factor to space of the radiator allowing more heat to be dissipated while minimizing the rise in vapor temperature.

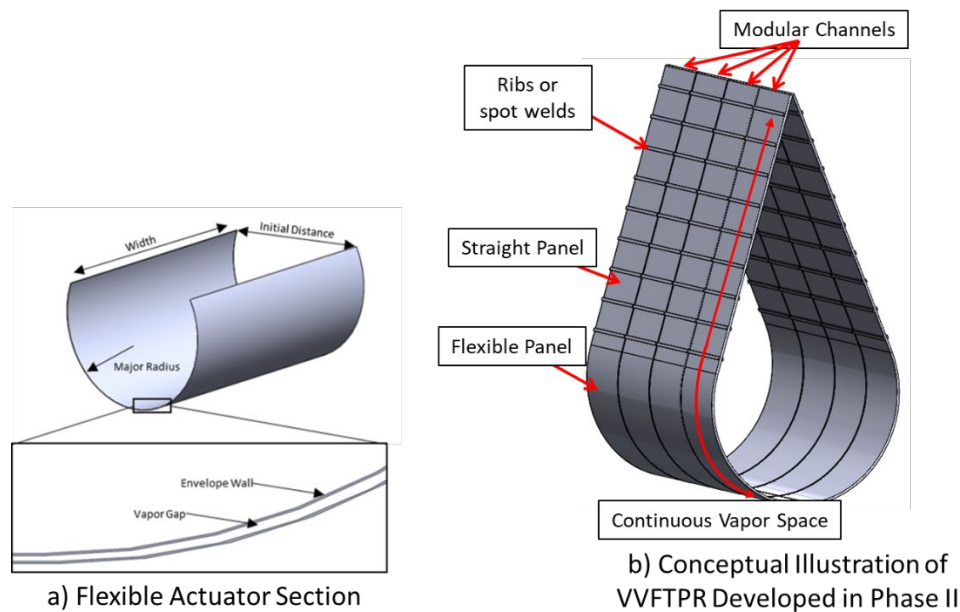


Figure 1. a) Illustration of flexible actuator section of the VVFTPR. b) Conceptual illustration of the VVFTPR design developed during the Phase II SBIR program.

During the Phase II SBIR program, ACT developed the conceptual design illustrated in Figure 1b which consisted of several key features:

- **Modular Channels:** The vapor space is divided into several modular channels along the span of the radiator as shown in Figure 1b. The channels are formed into a teardrop shape with a flexible curved actuator and two straight sections. The modular channels provide redundancy in the event of micrometeorite damage, by restricting potential leaks to a single module and not resulting in the loss of all of the working fluid.
- **Continuous Vapor Space:** The modular channels are constructed so that the flexible curved panel and the straight panels form a single continuous vapor space. By distributing two-phase working fluid throughout the entire channel an isothermal radiator can be achieved.
- **Structural Support:** Ribs or spot welds can be applied to the surface of the straight panel in order to contain the high internal pressure with a minimum wall thickness.

III. Manufacturing Method

This section summarizes the manufacturing steps taken to fabricate VVFTPR prototypes. This includes a description of the ultrasonic welding process, the material selection, heat treatment and the forming process to create the teardrop shape. During the program, a single-channel proof-of-concept prototype and a multi-channel radiator panel prototype with six individual channels were fabricated. Experimental testing is described in Section IV.

A. Ultrasonic Welding

During the Phase II SBIR program, ACT and EWI selected aluminum 7075 as the envelope material due to its high yield strength and low elastic modulus.⁵ Aluminum 7075 is prone to cracking when welded using traditional fusion welding techniques and it was decided to utilize ultrasonic welding. *Ultrasonic welding* is a solid-state weld process that joins the metal without melting allowing the material to retain its mechanical properties and avoids the potential for cracking. The method is capable of welding many metals that have traditionally been considered unweldable. Figure 2 shows an illustration of the ultrasonic welding setup. The two pieces to be joined are held together under pressure and high-frequency ultrasonic vibrations are locally applied. The combination of pressure, heat and friction leads to a solid metallic bond at the weld site. The process is easily automated and well suited to the production of the VVFTPR.

The ultrasonic welding process can easily be applied to form a radiator panel made of several individual channels using the weld pattern illustrated in Figure 3. The proposed design uses two continuous top and bottom sheets of the selected envelope material and the modular channels for vapor flow are formed by welding along the length of the sheets.

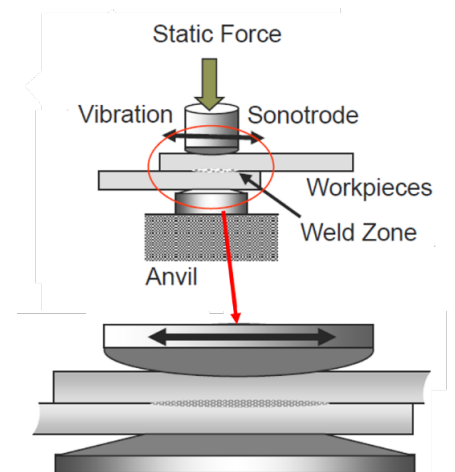


Figure 2. Illustration of the ultrasonic welding process. Source EWI.

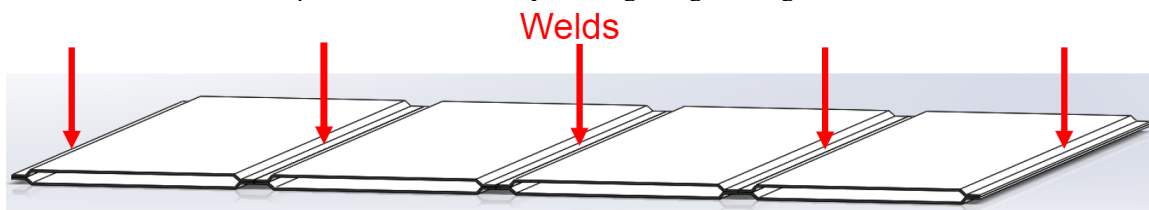


Figure 3. Welding pattern for multi-channel VVFTPR

After selecting the material and welding process, EWI performed a series of welding trials and experiments in order to down select an acceptable set of welding parameters. Parameters investigated during the trials included the sheet thickness, interlayer material thickness, brushed or not brushed surface, single or double weld pass, ultrasonic amplitude and weld force. Details of the weld development trials were presented by Diebold et al.⁵ A key finding of this development process was the need to utilize base material with an alclad layer. An alclad layer is a thin surface layer of pure aluminum that provides corrosion resistance to the base aluminum alloy. The alclad layer is typically 1-15% of the sheet thickness. Figure 4 shows a metallographic cross-section image, taken by EWI, of an aluminum 7075 sheet with an alclad layer.

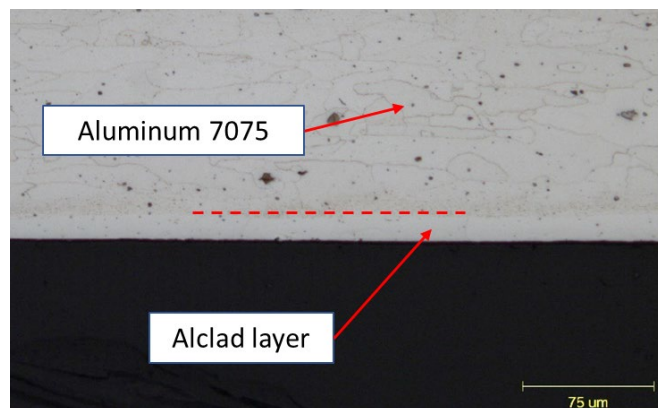


Figure 4. Metallographic cross-section image of a sheet of aluminum 7075 showing the alclad layer on the surface.

Attempting to directly ultrasonically weld aluminum 7075 to aluminum 7075 proved unsuccessful.⁵ Using

aluminum 7075 sheets with the alclad layer improved the weld quality because the alclad layer was significantly softer and easier to locally deform than the aluminum 7075. Based on the results of EWI's welding trials, all subsequent work was done with aluminum 7075 sheets with an alclad layer. The total thickness of the aluminum sheets used for prototype development was 0.012 in. The thickness of the alclad layer was 0.00078 in.

B. Heat Treatment Process

After finalizing the welding process, EWI worked to increase the strength of the weld by diffusing elements from the aluminum 7075 into the alclad layer via a heat treatment process. EWI conducted diffusion simulations using Thermo-Calc 2020a and the TCAL6 and MOBAL5 databases. The problem was setup as an asymmetrical closed system diffusion problem with a 0.01-in. aluminum 7075 layer with a 0.000787 in. alclad layer on one face. Symmetry existed at both the edges of the alclad layer and about the centerline of the aluminum 7075 so no mass movement occurred across these boundaries. A simplified composition for aluminum 7075 was used for this study of 90.4% Al, 1.5% Cu, 2.5% Mg, and 5.6% Zn as these are the primary strengthening elements in aluminum 7075. All percentages are mass %. The simulations were run at 480°C for varying times up to 4 hours.

Figure 5 shows the mass percent of copper through the base aluminum 7075 and alclad layers vs. location at several different times during the heat treatment. The concentration of magnesium and zinc throughout aluminum 7075 and alclad layer were also predicted but are not shown here. A significant amount of diffusion occurred over the first 90 minutes. The farthest portion of the alclad reaches about 50% of base material composition for CU and about 66% for Mg and Zn. These have higher mobilities in aluminum and therefore diffuse quicker. After four hours, the amount of Cu in the Alclad layer is 1.2% or about 75% of the base material composition, with Zn and Mg having slightly higher compositions. As this is diffusion, alloying elements were not created but rather extracted from the base material, slightly weakening the aluminum 7075. However, the trade-off for this application proved invaluable as it allowed forming of the part into the desired teardrop shape. This heat treatment was used for all single channel and full prototypes.

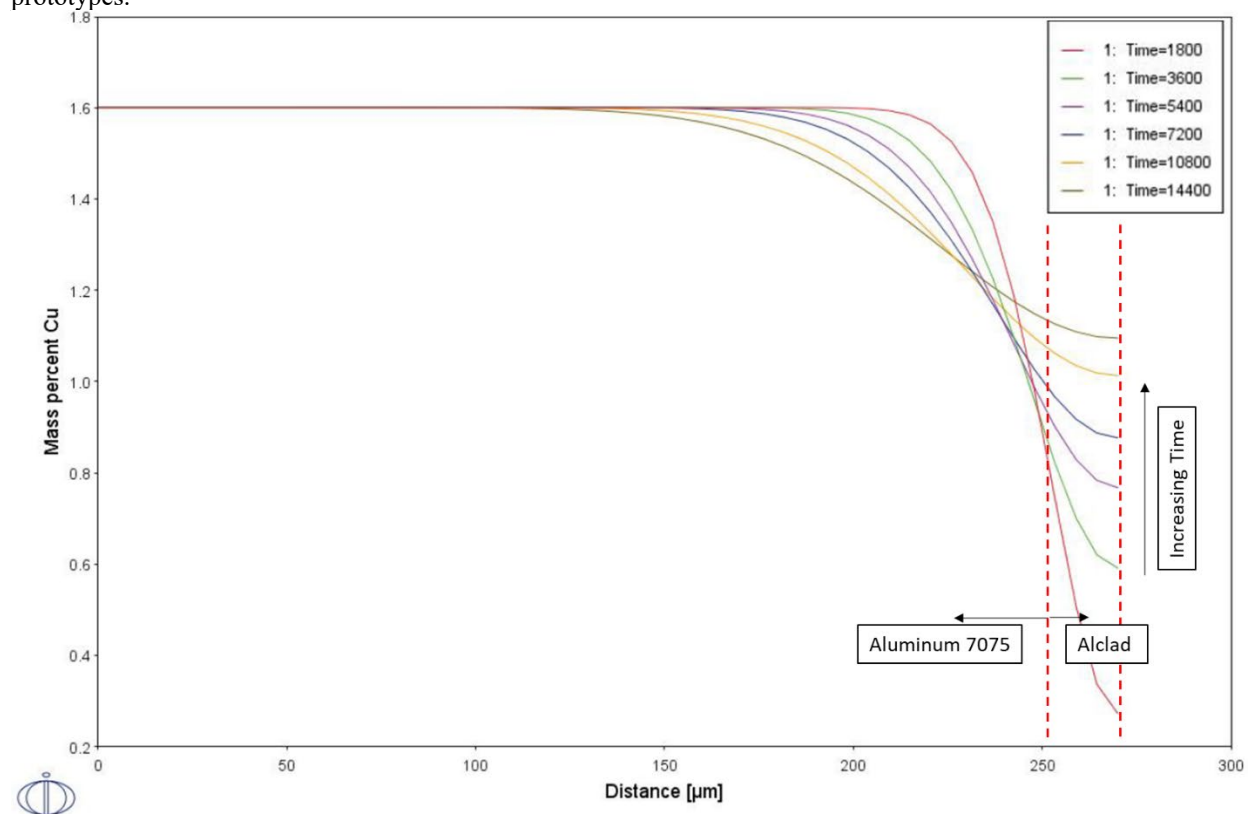


Figure 5. Results of diffusion simulation performed by EWI showing the mass percentage of copper in the base aluminum 7075 and the alclad layer as a function of location at several different times during the heat treatment. Aluminum 7075 layer was approximately 250μm thick and the alclad layer was 20μm thick. The temperature was 480°C.

Based on the results of the diffusion simulation it was decided to apply a heat treatment to all prototypes. While the heat treatment process strengthened the weld it also presented a new challenge due to warping that occurred while heating. Figure 6 compares images of ultrasonically welded aluminum 7075 single-channel prototypes before and after the heat treatment process. Note that the prototypes had spot welds on the areas that would become the straight sections after forming the teardrop shape, indicated in Figure 6a.

Warping resulted from residual stresses within the weld being relieved during the heat treatment. There are a few sources that likely caused a buildup of residual stress in the weldment. First, there was likely some residual stress in the sheet material from processing. Second, there was cold working/stress build up during the welding process. While the welding process was relatively cool, welded locations may heat to around 200°C. This would be expected to cause some mechanical deformation in the alclad layer and additional tension in the material as it is pushed through the seam welder. During heat treatment, this residual stress relaxed causing warping. Warping was also observed for the multi-channel prototype though the extent of warping was less.



a) Single-channel prototypes prior to heat treatment



b) Single-channel prototypes after heat treatment

Figure 6. Ultrasonically welded aluminum 7075 single-channel prototypes, a) prior to heat treatment and b) after heat treatment.

C. Initial Prototype Forming Step

After the heat treatment process, the prototypes were formed into the teardrop shape. This was a two-step process involving a press and die followed by a slip roller. A slip roller is a simple way to form the flat sheets into the desired teardrop shape; however, during the rolling process, the neutral axis of the prototype is located on the face that will be the inside of the teardrop. This results in large stresses on the weld and the opposite face of the envelope. Bending the flat prototype using a press and die places the neutral axis nearer to the center of the thickness of the envelope minimizing the stress on the weld. Figure 7 shows a sequence of images demonstrating the bending process for the multi-channel prototype. The large cylinder was selected to give the panel the desired bend radius of 4.0 in. The flat panels were loaded onto the frame (left) and then deformed at a rate of 0.5 m/min until the ends of the panels were vertical (center), and then the cylindrical die was removed (right). Ideally the press and die process would bend the panel beyond this vertical condition to a complete teardrop, but developing such a system was outside the scope of this work. An image of the prototype after being removed from the bending fixture is shown Figure 8. Unfortunately, after removing from the fixture significant spring back was observed. Spring back was also observed in the single-channel prototype but not to such an extent as for the multi-channel prototype. The reason for this is the additional weld seams increased the stiffness of the prototype resulting in higher tension on the outer sheet causing the panel to open back up. After the initial forming step, the prototypes were rolled into the final teardrop shape.



Figure 7. Sequence of images showing the initial bending step performed by EWI. Left – Panel loaded into test frame. Center – Panel Bend to 90°. Right – Center die removed from panel.



Figure 8. Panel after being removed from the bending fixture. After removing the panel from the bending fixture significant spring back was observed.

D. Final Single-Channel and Multi-Channel Prototypes

Figure 9 shows images of the final single-channel and multi-channel aluminum 7075 VVFTPR prototypes fabricated using the steps described above. Warping in the single-channel prototype was clearly evident. Fill tubes were installed on one straight section for each strip. The width of each channel was 1.25 in. The bend radius of the teardrop profile was 3.0 in. for the single-channel prototype and 4.0 in. for the multi-channel prototype. The multi-channel prototype was made of six separate channels.



a) Single-channel prototype



b) Multi-channel prototype

Figure 9. Images of the a) final single-channel prototype and b) multi-channel prototype.

IV. Experimental Testing

A. Single-Channel Prototype Testing

The single-channel prototype was fabricated first as a proof-of-concept for the manufacturing method described above. The single-channel prototype was tested by fixing the straight end with the fill tube and then pumping water into the channel. The internal pressure was measured with a pressure transducer and the opening distance was measured as shown in Figure 10. The experiment was carried out by increasing the pressure in small steps in order to identify where the prototype underwent plastic deformation. The pressure was set to a predetermined value and the opening distance was measured. The pressure was then released allowing the prototype to the relaxed state. If the prototype did not return to its original state this indicated that plastic deformation occurred. This process was repeated with increasingly higher values of pressure until plastic deformation occurred.

Figure 11 shows the experimental measurements for the single-channel prototype opening vs. internal pressure, simulation data is shown for comparison. Nonlinear 3D structural simulations were performed using Abaqus SIMULIA, see Diebold et al.⁴ for details. Note that when unpressurized, the experimental prototype had a slight opening of 1.5 in. This offset was subtracted from the opening measurements in Figure 11. The simulation predicted larger opening as a function of pressure until an internal pressure of approximately 8 psia. Experimental results were not acquired above this pressure because plastic deformation was observed above this point. The simulation exhibited higher sensitivity to pressure at low pressures compared to the prototype. It is important to note the relatively significant difference in the shape of the experimental prototype compared to the ideal teardrop shape of the simulation due to the warping described above, see Figure 6b. In addition, the experimental prototype had internal stress and was affected by work hardening, features that were not captured in the simulation.

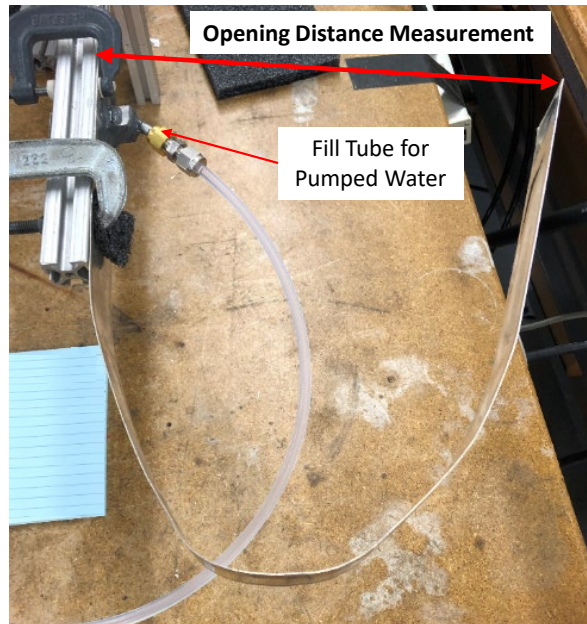


Figure 10. Single channel prototype in experimental setup. Internal gauge pressure = 7.91 psi. Opening Distance = 11.25 in.

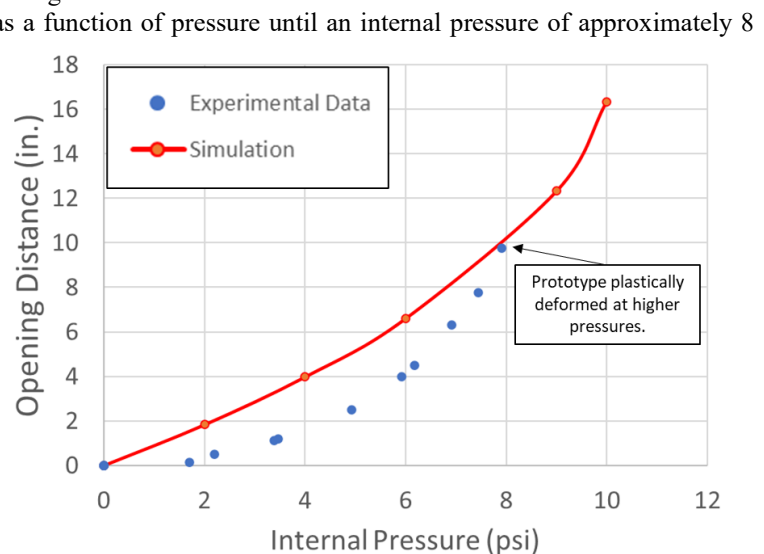


Figure 11. Comparison of experimental and simulation data for the single channel prototype. Wall thickness = 0.012 in. Bend radius = 3.0 in. At zero internal pressure, the experimental prototype had an opening of 1.5 in. this has been subtracted from all experimental measurements.

B. Multi-Channel Prototype Testing

While the single-channel prototype was only tested with pumped water, the intent of the multi-channel prototype was to demonstrate operation of the VVFTPR with a two-phase working fluid. Acetone was selected as the working fluid. Figure 12a shows an image of the multi-channel VVFTPR prototype with a rope heater and thermocouples attached. The rope heater was wrapped around the center of the prototype. Ideally, the VVFTPR panel would be fixed at the center of the profile (bottom of the teardrop) so that it would open symmetrically; however, due to the weight of the fill tubes and valves (seen in the upper left corner) it was necessary to support the prototype near the valves and allow the rest of the prototype to float, this is shown in Figure 12b. While not shown in Figure 12a, a rope heater was also wrapped around the valves and fill tube. Each of the 6 individual strips had 5 thermocouples (TC) located at points A-E indicated in Figure 12a. The strips were numbered 1-6 as indicated in Figure 12b. Each strip was charged individually with a predetermined amount of acetone.

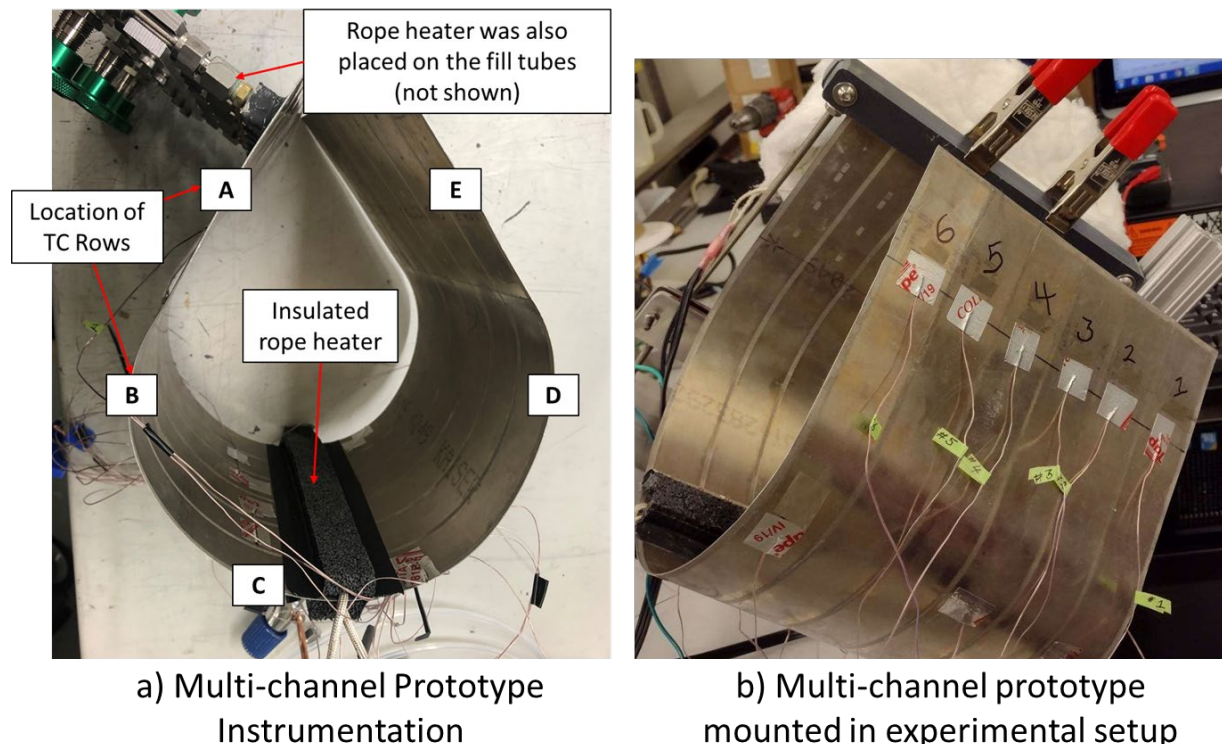


Figure 12. a) Image of the multi-channel VVFTPR with heater and thermocouples (TC) attached. Each strip had five TCs located at the positions marked A through E in the image, b) Image of the multi-channel VVFTPR prototype mounted in the test stand. The prototype was fixed at the end with the fill tube and valves in order to support the weight of the valves. The strips were numbered 1-6.

The initial testing with two-phase acetone proved unsuccessful. It was determined that the working fluid was trapped in the valves and fill tube and was not successfully penetrating into the channels. The fill tubes were placed very near to the spot welds within the straight section and the channel did not sufficiently open to allow the working fluid to fill the channel. To verify this, ACT modified the experimental setup to actively pump water into the multi-channel prototype, similar to the single-channel prototype. The pump allowed the pressure to build up sufficiently to push water into the channels. Two important observations were made during the pumped water test of the multi-channel prototype. First, as the pressure was increased the spot welds on the side of the prototype with the fill tubes began to fail. The failure of the spot welds allowed working fluid to more easily enter the channels and the prototype began to open in response to increasing internal pressure. The seam welds forming the channels did not fail. Second, the opening of the multi-channel prototype was asymmetric. This can be observed in Figure 13 which shows a top-down view of the multi-channel VVFTPR prototype during the pumped water test. The water entered the straight sections at the bottom left of the image and then began to travel in a clock-wise direction as indicated in the figure. The asymmetric opening can be observed by comparing the left and right-hand side of the curved section in the image.

The left-hand side, nearest the valves, had clearly undergone more deformation than the right-hand side. This indicated that while water was entering the channels it was not filling the entire length of the channel. In Figure 13, the water had only penetrated approximately half the length of the channels.

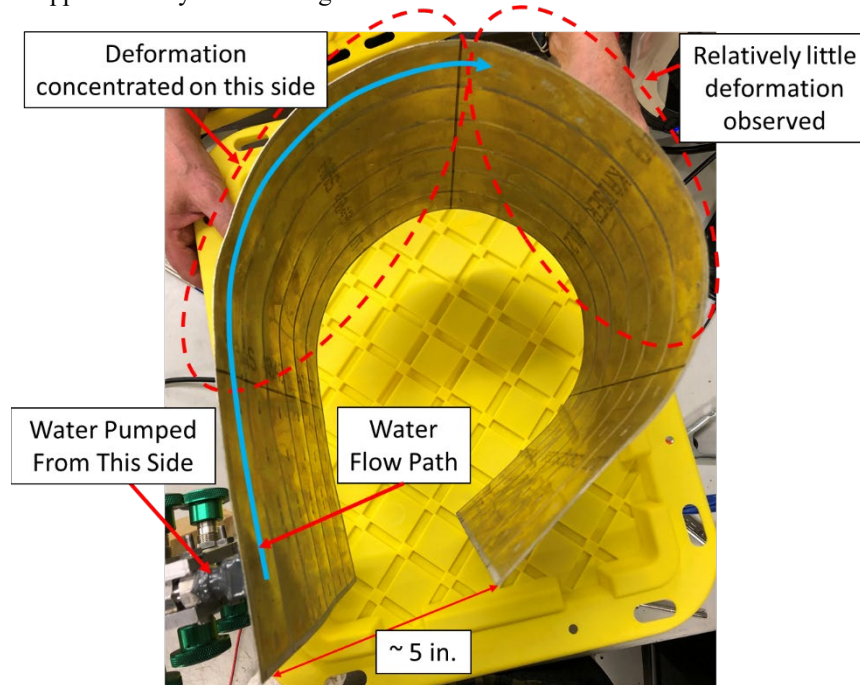


Figure 13. Image of the multi-channel VVFTPR prototype during pumped water testing. Internal pressure was approximately 25 psia. The image shows the asymmetry in the opening due to the water being pumped into the strips from one side and not fully penetrating the channels.

During the pumped water testing discussed above it was observed that many of the spot welds in the straight section failed, and it was suspected that the channels had undergone slight plastic deformation. It was hypothesized that this would allow acetone to penetrate from the valves further into the channels allowing the prototype to open in response to increasing vapor pressure due to heating at the center of the teardrop profile. In order to test this hypothesis, acetone was added back into all of the strips and a heater was attached to the center of the prototype. Figure 14 shows several images of the multi-channel prototype during testing with acetone. The heater was attached to the bottom of the teardrop shape. In the lower right-hand corner of each image a digital readout of a centrally located TC can be seen. A rope heater was also wrapped around the valves, not shown in Figure 14. The valve heater was turned on prior to the heater located in the center of the teardrop profile in order to force acetone out of the valves and into the channels.

The images of Figure 14 show the prototype at various stages of opening as the heater power was slowly increased and the central TC temperature increased from 52.2°C to 89.0°C. The opening was manually measured from fixed reference points on the prototype. The opening increased nonlinearly with temperature. As the prototype temperature increased from 52°C to 80°C (Figure 14a-c), the opening increased by only 2.5 inches. A slight increase in temperature from 80°C to 86.5°C (Figure 14d) resulted in the opening jumping an additional 5.65 inches, and a final increase in temperature from 86.5°C to 89°C (Figure 14e) resulted in an additional 1.15 inches of opening. The maximum opening measured, at 89°C, was approximately 13.25 in. It is difficult to create a direct relationship between the temperatures shown in Figure 14 and the measured opening because the heating rate of the valves was not the same as the prototype. As a result, some opening may be due to valve heating.

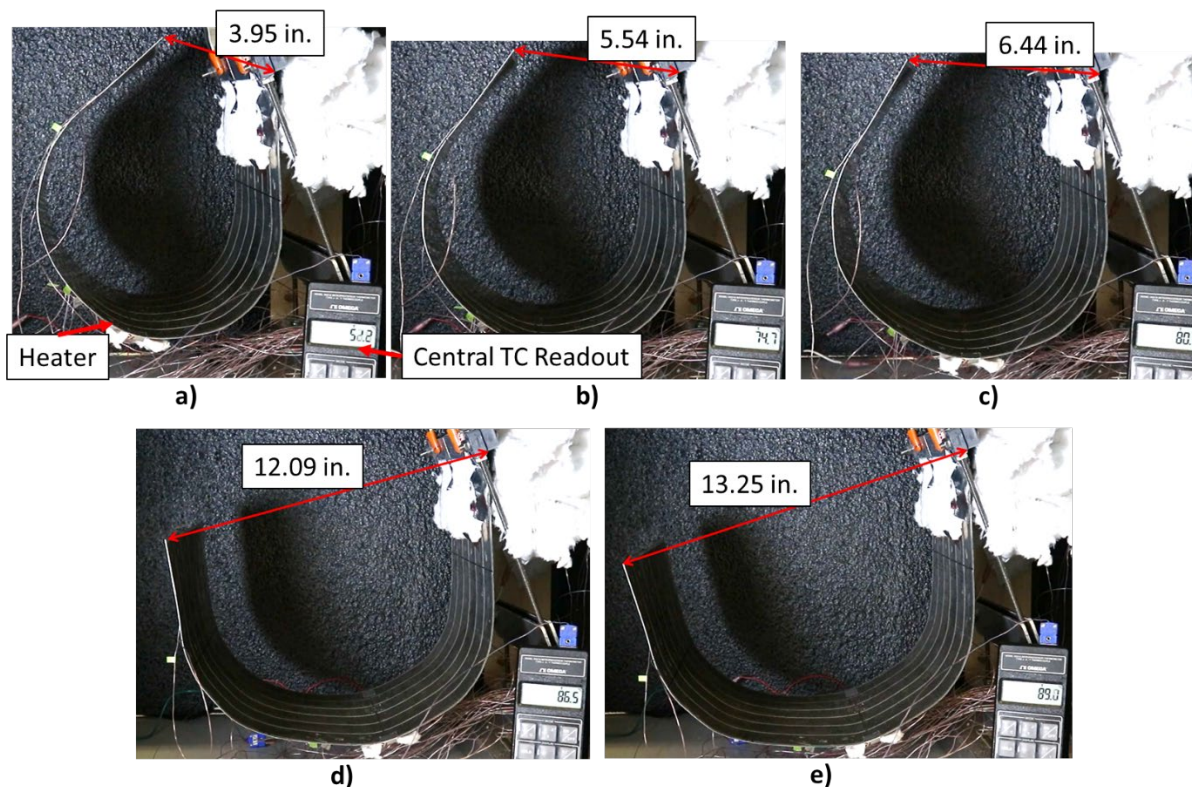


Figure 14. Results of two-phase acetone testing of the aluminum 7075 multi-channel VVFTPR prototype fabricated via ultrasonic welding. In the bottom right of each image a digital readout displays the temperature measured near the center of the prototype. The opening was manually measured at fixed reference points. The working fluid was acetone.

While difficult to see in Figure 14, it was observed that the side of the prototype with the valves underwent more deformation than the free end. This was similar to what was observed in the pumped water test, shown in Figure 13. This suggests that the working fluid was still not able to fully penetrate the entire length of the channel. This was supported by temperature measurements along the length of the strips. Table 1 shows the temperature at points A-E, which were defined above in Figure 12a, on Strip 3 at a point in time corresponding to the maximum opening shown in Figure 14. Points B and D were located symmetrically about the heater, in the curved section of the prototype, and both indicated similar temperatures. Points A and E were located in the straight section, also symmetrically about the central heater, but Point A was approximately 30°C hotter than Point E indicating that no acetone was reaching Point E. Point E was only heated by conduction through the envelope. It is likely that the spot welds on the free-end of the prototype had not yet failed and were blocking the progress of acetone.

Table 1. Temperature measurements at Points A-E (see Figure 12a) of Strip 3 at the maximum opening shown in Figure 14e.

TC	Description of Location	Temperature
A	Straight Section, Valve Side	61.4°C
B	Curved Section, Valve Side	63.7°C
C	Center, Near Heater	91.1°C
D	Curved Section, Free End	61.0°C
E	Straight Section, Free End	34.4°C

The results shown in Figure 14 represent the first successful test of the aluminum 7075 ultrasonically welded VVFTPR concept. The prototype successfully opened in response to heating of an internal two-phase fluid and the resulting rise in vapor pressure.

V. Conclusion

Under a NASA Phase II SBIR program, ACT in collaboration with EWI developed and experimentally demonstrated a variable-view-factor two-phase radiator with an aluminum 7075 envelope fabricated via ultrasonic welding. The manufacturing process involved ultrasonically welding the desired prototype, a heat treatment to strengthen the weld, an initial bending step with a press and die setup and a final rolling step to achieve the desired teardrop shape. Experimental testing successfully demonstrated the operation of a multi-channel VVFTPR prototype with a two-phase working fluid. The prototype was able to achieve significant changes in geometry in response to increasing vapor pressure of the internal two-phase fluid. These results mark the end of the Phase II SBIR program. Recommendations for future work include:

- Modifications to the welding fixture may reduce the tensile effects between the two sheets of the material during welding. This would reduce the residual stress in the material and reduce the warping that occurred during the heat treatment process.
- Warping during the heat treatment can also be reduced through the use of a fixture for the part while the heat is applied.
- The initial bending step should be improved. Possible alterations worth investigating are:
 - Hot forming of the material
 - Iterative radius development
 - Use of an upper and lower die rather than the three-point bend method shown in Figure 7
- During fabrication a spacer should be included within the channel to separate the walls of the envelope. Spacers would allow fluid to evenly distribute throughout the channels, even at low pressures significantly improving the opening of the radiator.

Acknowledgments

This project was funded by NASA Marshall Space Flight Center under a SBIR Phase I program (Contract 80NSSC18P2187) and Phase II program (Contract 80NSSC19C0209). ACT would like to thank our technical monitor, Jeff Farmer. In addition, special thanks are due to Larry Waltman, Philip Texter, Eugene Sweigart and Tyler Spinello, the technicians who supported the program at ACT.

References

- ¹ Viswanatha, N. and Murali, T., "A Novel Mechanism using Shape Memory Alloy to Drive Solar Flaps of the INSAT-2E Satellite," Proceedings of the 34th Aerospace Mechanisms Symposium, pp. 241–251, 2000.
- ² Christopher L. Bertagne, Rubik B. Sheth, Darren J. Hartl, and John D. Whitcomb, "Simulating Coupled Thermal Mechanical Interactions in Morphing Radiators," Proceedings of the SPIE, Volume 9431, 94312F, 2015.
- ³ Lutz, A., Tarau, C. and Rokkam, S., "Variable-View-Factor Two-Phase Radiator", ICES-2019-211, 49th International Conference on Environmental Systems, 2019.
- ⁴ Diebold, J., Tarau, C., Lutz, A. and Rokkam, S., "Development of Variable-View-Factor and Deployable Two-Phase Radiator," ICES-2020-317, International Conference on Environmental Systems, 2020.
- ⁵ Diebold, J., Tarau, C., Lutz, A., Rokkam, S., Eff. M. and Lindamood, L., "A Variable-View-Factor Two-Phase Radiator Manufactured Via Ultrasonic Welding," ICES-2021-260, 50th International Conference on Environmental Systems, 2021.